ELSEVIER

Marine Chemistry 80 (2002) 41–59

MARINE CHEMISTRY

www.elsevier.com/locate/marchem

The distribution of Mo, U, and Cd in relation to major redox species in muddy sediments of the Bay of Biscay

Gwénaëlle Chaillou*, Pierre Anschutz, Gilbert Lavaux, Jörg Schäfer, Gérard Blanc

Université Bordeaux 1, D.G.O. UMR 5805 CNRS, Avenue des Facultés, 33405 Talence Cedex, France

Received 4 June 2001; received in revised form 7 August 2002; accepted 7 August 2002

Abstract

In order to understand the relationship between authigenic precipitation of U, Mo, Cd, and the redox properties of the marine environment, we have studied the vertical distribution of these metals and of the major redox species (oxygen, nitrate, manganese, reactive iron, sulfate, carbon, and sulfur) in modern sediment. We have sampled four sites at 150 to 2800 m depth in the Bay of Biscay. At the shallowest station, where sediment is highly bioturbated, organic carbon levels are above 2% and particulate sulfides are abundant. At the deepest stations, sediment is much less bioturbated, and organic carbon levels are lower. At all sites, early diagenesis follows a well-established depth sequence of redox reactions, based on the bacterially mediated oxidation of organic matter. Manganese-oxides and authigenic U and Mo were extracted by an ascorbate solution. Molybdenum is associated with these oxides in the oxic part of cores. In the anoxic layer of the sediment, Mo precipitates as a detectable authigenic phase only when sulfide minerals are present, i.e. when sulfate reduction becomes important. In anoxic sediments, Cd enrichment is a good indicator of sulfide production from sulfate reduction even if the production is weak. Uranium precipitates at the depth of reactive iron (III) reduction. No relationship was observed between U and S. The U concentration at the depth of precipitation agrees with values calculated using estimated accumulation rates and a downward diffusive flux of dissolved U from the bottom seawater into the sediment. However, authigenic U concentrations continue to increase in the anoxic part of the cores. Therefore, it is difficult to establish a direct relationship between the process of U accumulation and the flux of C_{org} to the sediment.

Keywords: Molybdenum; Uranium; Cadmium; Early diagenesis; Sediment; Bay of Biscay

1. Introduction

The pattern of accumulation of redox-sensitive metals in marine sediments is thought to reflect oceanic productivity represented by a flux of organic matter to the seafloor. The distribution of these metals in marine sediments can be used to determine bottom water redox conditions at the time of deposition. This information allows us to define areas where the flux of organic carbon exported to the sediment was important.

Uranium and molybdenum are two interesting proxies of redox conditions in marine sediments, because they are conservative in the oxygenated ocean and enriched in anoxic sediments (Bertine, 1972;

* Corresponding author. Tel.: +33-5-56-84-88-73; fax: +33-5-56-84-08-48.

E-mail address: g.chaillou@geocean.u-bordeaux.fr (G. Chaillou).

0304-4203/02/$ - see front matter © 2002 Elsevier Science B.V. All rights reserved.
PII: S0304-4203(02)00097-X

François, 1988). Their valence and solubility vary as a function of redox potential (Calvert and Pedersen, 1993). Cadmium is also interesting: it exhibits a nutrient-like distribution in the oxygenated column but is enriched in sulfidic sediments, where it forms highly insoluble sulfides (Rosenthal et al., 1995).

In order to improve paleoceanographic interpretations based on the sedimentary metal distribution, it is necessary to understand geochemical behaviour during early diagenesis. Therefore, we have studied the distribution and authigenesis of U, Mo, and Cd in modern sediments. The thickness of the oxic layer defines the diffusive gradient of dissolved metal between bottom water and the anoxic part of the sediment, where metals precipitate. The flux of metals, i.e. the amount of authigenic U, Mo, and Cd, is function of the O_2 penetration in the sediment (Gobeil et al., 1987; Thomson et al., 1990; Martinez et al., 2000). Recent studies have revealed a more complex behaviour of redox-sensitive trace metals. For example, trace metals can interact strongly with metal oxides in the oxic sediment layer, and with sulfides in the anoxic layer. The depth where metals precipitate is not necessarily identical to the depth of O_2 penetration, because species such as NO_3^- or Mn-oxides, present deeper in the sediment, can be oxidants for trace metals. Therefore, the redox stratification of sediments is not simply restricted to a surficial oxic and a deeper anoxic layer. Furthermore, bioturbation can redistribute chemical species in the sediment, by transporting trace metals associated with particulate material across redox gradients.

The vertical degradation sequence of organic matter proceeds by a sequential consumption of electron acceptors during oxidation of organic carbon (C_{org}) according to the energy yield per unit of reactive organic matter. Reduction of oxygen near the sediment/water interface is followed by reduction of nitrate, manganese- and reactive iron-oxides, sulfate, and, finally, carbon dioxide (Froelich et al., 1979; Postma and Jakobsen, 1996). In this study, we present vertical profiles of total, extractable, and dissolved trace metals as well as major components of the redox system. Early diagenesis yields reduced products and creates chemical gradients and fluxes. The processes involved in reoxidation of reduced products, particularly of N, Mn, Fe compounds, is still a matter of debate (Hulth et al., 1999; Anschutz et al., 2000; Hyacinthe et al., 2001) and can contribute to the distribution of trace metals. This study is based on four sediment cores collected between 150 and 2800 m depth on the Aquitaine margin in the Bay of Biscay (France). The four sites differ in terms of organic matter content, sedimentation rate, and bioturbation intensity. This study is a part of the program Oxybent, which focuses on the mechanisms of benthic biogeochemistry and their role in the fossilisation of sedimentary signals.

2. Material and methods

2.1. Sampling location

Sediment samples were collected in June 1999 during cruise Oxybent 9. Undisturbed sediment cores were collected between 150 and 2800 m depth in the southeastern part of the Bay of Biscay on the slope of the Aquitaine margin (stations A, B, and D), and close to the canyon of Cap Ferret (station I; Fig. 1). The sediments of the stations located above 700 m (D and B) are in contact with North Atlantic Central Waters, whereas station A is under the influence of a layer of Mediterranean waters (Table 1). The temperature of both water masses range from 10.5 to 13 °C. The bottom of station I is overlaid by North Atlantic Deep Waters, with a temperature of 4 °C.

2.2. Material

Cores were collected with a multicorer, which allows the sampling of sediment/water interface sampled with minimum disturbance. Grain size was measured using a laser diffractometer (Malvern Mastersizer). Overlying water was collected immediately after core recovery for dissolved O_2 measurements, using the Winkler titration method (Strickland and Parsons, 1972). Profiles of pore water O_2 were measured on board using a cathode-type mini-electrode (Revsbech, 1983; Helder and Backer, 1985; Revsbech and Jørgensen, 1986). The temperature was maintained constant with an insulating device. This operation was completed within 15 min after core recovery for sediments where the oxygen penetration depth was lowest, and within 30 min for other cores. Subsequently, the core used for O_2 profiling was sliced in thin horizontal

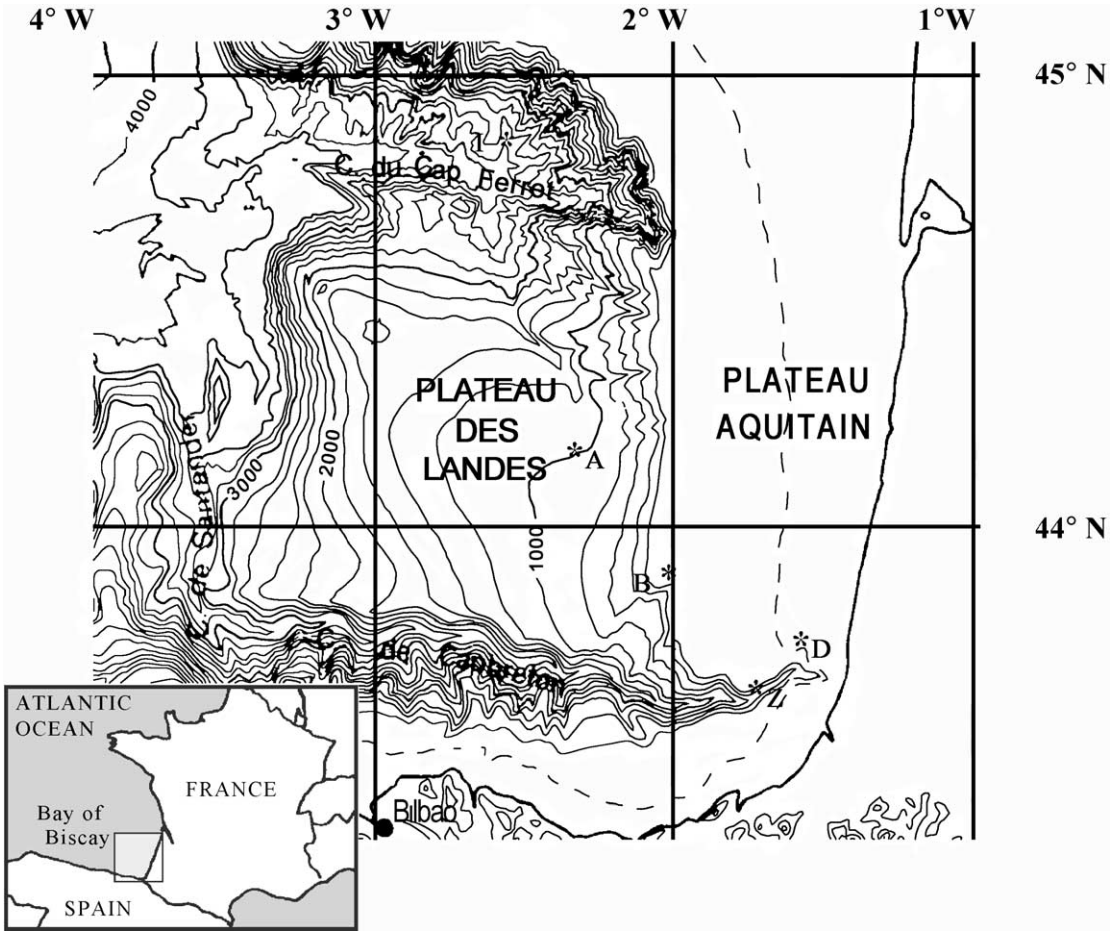

Fig. 1. Map of the southeastern part of the Bay of Biscay showing the location of Oxybent 9 cruise stations.

sections (0.5 cm for the top 2 cm, 1 cm below, and 2 cm at the bottom) within 1.5 h. A subsample of each slice was immediately sealed in a preweighed vial and frozen under inert atmosphere (N_2) for later determination of porosity. Another subsample was centrifuged under N_2 at 5000 rpm for 20 min to extract pore water. Two aliquots of water were filtered (0.2 μm, syringe filter SFCA purged with N_2) and frozen at -25 °C for nutrient analysis, and a third aliquot was filtered and acidified to pH 1.6 with ultrapure HNO_3 for dissolved Mn and Fe analysis. Eliminating oxygen contamination completely during pore water extraction is difficult. Despite the precautions taken, we cannot exclude the possibility that traces of oxygen may have affected the pore water concentrations of redox-sensitive elements during slicing of cores and the filtration.

Surface sediments from a second core were collected for ^{210}Pb and ^{234}Th analysis. The complete vertical profiles of ^{210}Pb and ^{234}Th activities for stations A, B, and D were obtained in cores collected at the same locations during mission Oxybent 1 (Anschutz et al., 1999). We noted the presence of polychaetes and burrows down to 40 cm at station D. At all the stations, the sediment consisted of mud composed of clay, silt, and less than 30% carbonates.

2.3. Laboratory analyses

The maximum sedimentation rates and the thickness of the mixed layer of the sediment were estimated from vertical profiles of excess ^{210}Pb and excess ^{234}Th ($^{210}Pb_{xs}$, $^{234}Th_{xs}$). The activities of radiogenic iso-

Table 1
Some properties of the studied stations (Oxybent 9)

	Station I	Station A	Station B	Station D
Geographic position	44°49′00N	44°10′00N	43°50′00N	43°42′00N
	2°33′00W	2°22′00W	2°03′00W	1°34′00W
Depth (m)	2800	1000	550	150
Temperature (°C)	4	12	12	12.5
O_2 bottom water (μmol/l)	253	200	215	235
$\%C_{org}$ interface	1.39	1.51	1.83	2.32
$\%C_{inorg}$ interface	2.75	3.37	2.12	1.59

topes, ^{210}Pb (half-life = 22.4 years) and ^{234}Th (half-life = 24.1 days), were determined in freeze-dried samples of about 5 g each, sealed in a counting vial, by a high-resolution and low-background gamma spectrometer with a semiplanar detector for at least 12 h (Jouanneau et al., 1988). Supported ^{210}Pb was determined by three independent methods, which gave the same result within the counting errors. It was estimated first from the average of ^{210}Pb activities in deeper sections of the cores (except for station D). Second, ^{226}Ra-supported ^{210}Pb activities were estimated from direct measurements of ^{226}Ra activities by gamma counting, and third, ^{226}Ra activities were obtained from ^{214}Bi and ^{214}Pb. ^{226}Ra activities did not vary greatly within the cores. The mean values of ^{226}Ra-supported were 24.3, 25.9, 32.45, and 48.3 Bq/kg for the stations D, B, A, and I, respectively. These data were significantly lower than the total ^{210}Pb activities, where $^{210}Pb_{xs}$ were reported (Fig. 2), suggesting a minimal error in the profiles of $^{210}Pb_{xs}$. Supported ^{234}Th activities were determined from average activities in deep layers of the sediment cores, and by recounting some surface samples after more than 1 year. Porosity was determined from weight loss upon freeze-drying. The freeze-dried solid fraction was homogenised for solid-phase analysis. The water content was used to correct these analyses for the presence of sea salt.

2.3.1. Solid phase analyses

Total element concentrations were determined from 30 mg freeze-dried samples that had been completely digested in a mixture of 2 ml HF, 250 μl HNO_3 70%, and 750 μl HCl 30% according to the procedure described by Loring and Rantala (1992). The final solution consisted of 1% HNO_3 solution with a water/sediment ratio of 500. Sediment was also extracted with an ascorbate solution, in order to extract the most reactive part of Fe (III) phases and all Mn (III, IV)-oxides and oxyhydroxides, and the co-precipitated or adsorbed trace metals associated with these metal oxides. The ascorbate solution also

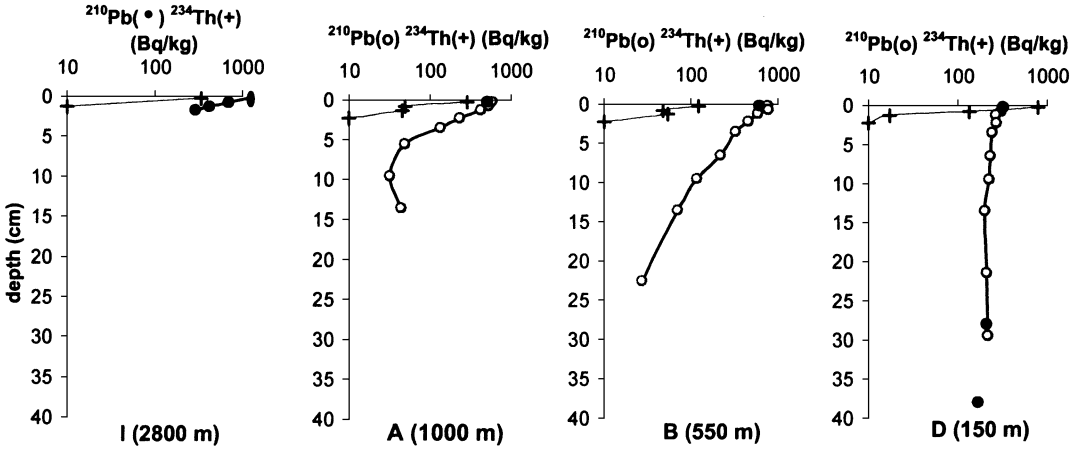

Fig. 2. Vertical profiles of log $^{210}Pb_{xs}$ and log $^{234}Th_{xs}$ in Bq/kg. The $^{210}Pb_{xs}$ profiles of stations A, B, and D (open dots, ○) were obtained from cores collected during the mission Oxybent 1 (October 1997). The black dots (●) represent the log $^{210}Pb_{xs}$ of surface sediments collected during Oxybent-9 (June 1999). The crosses (+) represent the log $^{234}Th_{xs}$ profiles of surface sediments collected during Oxybent 9.

dissolves partially Fe monosulfides (Kostka and Luther, 1994; Anschutz et al., 1998; Hyacinthe et al., 2001). About 1 g of wet sediment was leached during 24 h with 25 ml of an ascorbate reagent consisting of 50 g of $NaHCO_3$, 50 g sodium citrate, and 20 g ascorbic acid in 1 l H_2O with a final pH of 8. Aliquots of centrifuged solution were then diluted to obtain 0.2 M HCl for Fe and Mn analysis and 1% HNO_3 for trace metal analysis.

Iron and manganese were analysed using flame atomic absorption spectrometry. The precision estimated from replicates was ± 3% for Mn and ± 7% for Fe. Accuracy was better than 10%. Trace metals were determined using Inductively Coupled Plasma-Mass Spectrometry (ICP-MS, ELAN 5000; Perkin-Elmer). The applied analytical methods were continuously quality checked by the analysis of international certified reference materials (MESS-2 and SL-1): accuracy was within 14% for Mo, 7% for U, 8% for Cd, and precision was generally better than 10% for concentrations 10 times higher than detection limits.

Particulate organic carbon (C_{org}), total carbon, and sulfur (S_{tot}) were measured on freeze-dried samples by infrared spectroscopy using a LECO C-S 125. Particulate organic carbon was measured after removal of carbonates with 2 M HCl from 50 mg of powdered sample. Inorganic carbon is the difference between total carbon and particulate organic carbon. Inorganic carbon was also measured by calcimetry giving identical results. The precision of these analyses was ± 3 μmol/g.

2.3.2. Pore water analyses

Dissolved nitrate ($\Sigma NO_3^- = NO_3^- + NO_2^-$) and NH_4^+ were analysed by Flow Injection Analysis (FIA), according to the procedures described by Anderson (1979) and Hall and Aller (1992). The precision was ± 0.5 μmol/l for ΣNO_3^- and ± 5% for NH_4^+. Dissolved Mn (acidified pore water samples) was directly measured by flame atomic absorption spectrometry. Dissolved Fe was analysed with the ferrozine procedure described by Stookey (1970). The precision was ± 10%. Sulfate was measured with a nephelometric method.

Dissolved trace metals were analysed in acidified pore water by ICP-MS after dilution (1:20) in 1% HNO_3 solution. The applied analytical methods were continuously quality checked by the analysis of an international certified reference material (SLRS-4). Multipoint calibrations were applied for all the elements studied. Working standards were prepared daily by diluting ready-to-use Analab standards. Matrix effects due to the salinity have been reduced by dilution (20-fold; dissolved charge < 1.8 ‰), and were checked by measuring representative samples using the standard addition method. Results obtained by external calibration and standard addition were compatible (~ 2%). Isobaric interferences have been checked for Mo and U by measuring different isotopes (^{95}Mo, ^{97}Mo, ^{98}Mo, and ^{238}U) and can be excluded. Pore water Cd (isotopes ^{112}Cd and ^{114}Cd) has been analysed, but the concentrations in all samples were below the detection limit of the ICP-MS (concentrations < 300 pmol/l).

3. Results and discussion

3.1. Activity of $^{234}Th_{xs}$ and $^{210}Pb_{xs}$, and the flux of particles

The excess activity of ^{234}Th in the four cores decreased rapidly below the water/sediment interface (Fig. 2). The activity of $^{234}Th_{xs}$ was below the detection limit at 1 cm depth at the station I, and below 2 cm depth at the stations B and A. At station D, $^{234}Th_{xs}$ was detected even at 4 cm depth. The presence of $^{234}Th_{xs}$ in the surficial sediments suggests that we have collected fresh deposit sediments and that the water/sediment interfaces were conserved during sampling. Because the half-life of $^{234}Th_{xs}$ is short in relation to the rate of burial due to simple sedimentation, its occurrence below the sediment interface suggests that bioturbation occurred in the studied sediments. At station D, the occurrence of activity of $^{234}Th_{xs}$ below the oxic layer (5 mm) and down to 4 cm suggests an important biological mixing. The absolute values of $^{234}Th_{xs}$ in the surface sediment were different in October 1997 (Oxybent 1 cruise) and in June 1999 (Oxybent 9 cruise; Fig. 2). This indicates the $^{234}Th_{xs}$ flux and/or the mixing intensity of the sediment changed with time.

The excess activity of ^{210}Pb decreased exponentially below the interface at the deep slope stations (I, A, and B; Fig. 2). The $^{210}Pb_{xs}$ activities of surface sediments measured in cores from Oxybent 9 were close to those measured during previous Oxybent

cruises, which suggests that the flux was constant. In the absence of bioturbation, the depth distribution of $^{210}Pb_{xs}$ permits the dating of the sediment over a recent time period. However, in the studied sediments, where particle mixing by the macrofauna occurs, the profile of $^{210}Pb_{xs}$ is subject to disturbance by burrowing organisms, and may only yield a maximum value for the accumulation rate (Silverberg et al., 1986; Thomson et al., 2000). The exponential decrease of activity of $^{210}Pb_{xs}$ at the deep slope stations (I, A, and B) suggests that the maximum accumulation rate was constant over time (Fig. 2). The maximum sedimentation rates deduced from the slopes of the $^{210}Pb_{xs}$ profiles, and the radioactive decay constant, are 0.033, 0.068, and 0.15 cm/year for stations I, A, and B, respectively. The maximum accumulation rates deduced from these sedimentation rates, the porosity, and the density of particles for stations B, A, and I, are 79.5, 36, and 17 mg/cm^2/year, respectively.

The $^{210}Pb_{xs}$ profile was almost vertical at station D, and exhibited only a small decrease from 320 to 168 Bq/kg at 40 cm depth (Fig. 2). A sediment core collected at the same location was radioradiographied using a Scopix system (Migeon et al., 1999), which consists of an X-ray imaging system combined with image analysis software. The image of the station D exhibited unlaminated sediment, with no evidence of slumping structures, and a lot of burrows and galleries down to the bottom of the sediment section, which suggests strong biological activity far below the oxic layer. The presence of polychaetes and numerous active burrows observed during sampling, down to several decimetres depth at this station, supports also this hypothesis. The maximum sedimentation rate calculated from the $^{210}Pb_{xs}$ profile is about 2 cm/year. This value is probably far from the real sedimentation rate, because the shape of the $^{210}Pb_{xs}$ profile is obviously influenced by biological mixing of particles. Such a shape of $^{210}Pb_{xs}$ profile has been already observed by Aller et al. (1998) in hemipelagic sediments of the Panama Basin (~ 3900 m): despite an O_2 penetration of 7 mm, the $^{210}Pb_{xs}$ profile was almost vertical down to 20 cm. This profile was interpreted as high sediment rate with high bioturbation (Aller et al., 1998). It is likely that the accumulation rate at the station D is higher than that of the others, because this station is the shallowest, located near the continent, and the most enriched in C_{org}.

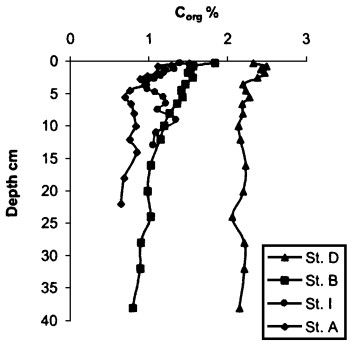

Fig. 3. Vertical profiles of pore water oxygen in μmol/l for stations D, B, A, and I.

The surface sediment C_{org} concentration (Fig. 3) decreased from the shallowest station D (2.32%) to the deepest station I (1.39%). At stations I, A, and B, the C_{org} content decreased slowly down core. It remained approximately constant at station D. The C_{org} content of surficial sediments are positively related to the calculated maximum accumulation rates as suggested by Calvert (1987). Consequently, we can estimate that the C_{org} flux at the sediment/water interface decreases as D≫B>A>I.

3.2. The distribution of the major species reacting during early diagenesis

3.2.1. Description of the concentration vs. depth profiles

The penetration depth of dissolved O_2 ranged between 5 mm at station D and 50 mm at station I (Fig. 4). The profiles of stations I and A showed a sharp O_2 gradient in the top 5 mm, and below, a smoother decrease until total anoxia. The concentrations of nitrate in the bottom waters of stations A and I were 15 and 20 μmol/l, respectively. Nitrate concentration was lowest at the shallowest station (Figs. 5–8). The top sample of the pore water profiles was enriched in NO_3^- relative to the bottom water, suggesting that the sediment was a source of nitrate for the water column in June 1999. Nitrate dropped to concentrations close to zero below the oxic layer. However, NO_3^- was sporadically present in the anaerobic part of the sediment. The NO_3^- profile of station I (Fig. 8) shows a maximum concentration in the oxic layer at 1 cm depth. Below which, the concentration

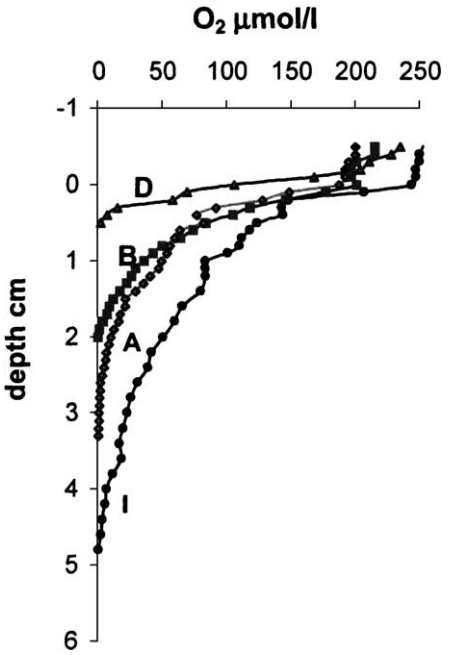

Fig. 4. Vertical profiles of C_{org} in weight % of the whole rock for stations D, B, A, and I.

decreased irregularly. Dissolved NH_4^+ concentrations were below the detection limit in the bottom water and remained low in the oxic part of the sediment (Figs. 5–8). They increased generally in a regular manner just below. The concentrations were highest at the bottom of the cores and at the station enriched in C_{org}.

Dissolved manganese, Mn (II), became detectable in samples where the oxygen concentration reached values close to zero (Figs. 5–8). Below this, the Mn (II) concentrations increased gently with depth at station I. At stations A, B, and D, the Mn (II) profiles showed a peak below the oxic layer (13, 25, and 43 μmol/l, respectively). Below the peak, the concentration decreased towards lower but constant values. Dissolved iron, Fe (II), appeared deeper than dissolved manganese, at a depth corresponding to the disappearance of NO_3^- (Figs. 5–8). The profiles of Fe (II) were more noisy than those of Mn (II). Sulfate concentration remained close to seawater concentration in the two deepest stations. The SO_4^{2-} profiles exhibited a slight decrease with depth at station D and to a lesser extend at station B (Figs. 5–8). Dissolved sulfide has not been analysed, but the concentrations were probably quite low, for we noted no smell of sulfide during core processing.

The profiles of Mn_{asc} and Mn_{tot} are parallel. Total Mn in the anaerobic part of the cores was between 4 and 10 μmol/g (Figs. 5–8). Solid Mn was higher in the oxic layer than in anoxic part of sediments (Figs. 5–8). The difference in particulate Mn corresponded to the Mn extracted by the ascorbate solution, indicating that it was present as Mn-oxides. The top of station D also showed high Mn-oxides concentrations, but the enriched layer extended even a few cm below the oxic front (Fig. 5). The shape of the Fe_{asc} profile, corresponding to poorly crystallized Fe (III) species, was similar to the profile of Mn_{asc} for stations I, A, and B (Figs. 6–8). Ascorbate-extractable Fe reached low constant values at the depth where dissolved Fe^{2+} first appeared in the pore water. The Fe_{asc} profile of station D was relatively linear in the whole core.

3.2.2. Early diagenetic processes

The distribution of major redox species showed the same pattern in the four studied cores. Oxygen concentration decreased rapidly below the sediment surface. Nitrate increased in the oxygen containing layer and then decreased below. The disappearance of oxygen and nitrate was accompanied by a decline of the Mn-oxide content and an increase in dissolved Mn, followed deeper down by an increase in dissolved Fe. Dissolved sulfate decreased with depth in the cores B and D. This distribution follows the well-established depth sequence of diagenetic reactions governed by the preferential use of the electron acceptor that yields the highest amount of free energy for the bacterially mediated oxidation of organic matter. Oxygen is reduced near the sediment/water interface, followed by the reduction of nitrate and manganese-oxide, then reactive iron-oxide (Fe_{asc}), and sulfate (Froelich et al., 1979; Postma and Jakobsen, 1996).

The O_2 consumption is attributed to oxic degradation of organic matter and the reoxidation of the reduced products from the anaerobic degradation of organic matter (Canfield et al., 1993). The observed thickness of the oxic layer depends directly on the C_{org} flux transport to the sediment surface. The peak of nitrate in the oxic layer is attributed to the succession of reactions that lead to the bacterial nitrification of organic N or ammonia diffusing from below. The consumption of nitrate below the oxic layer is due to

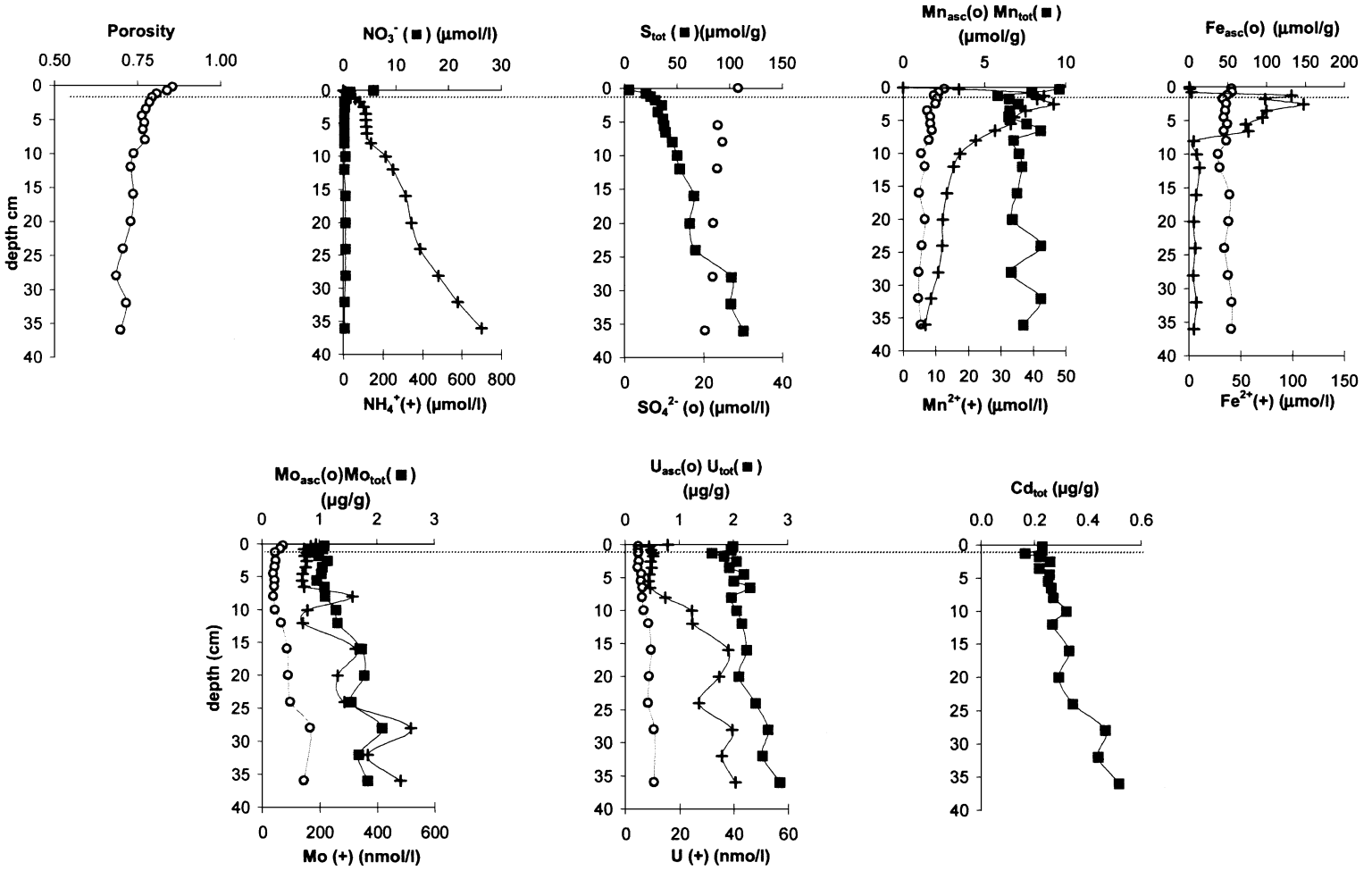

Fig. 5. Vertical distribution of redox species in pore waters and in the solid fraction as determined from total digestion and ascorbate leaching in the core of station D (150 m). The dashed line represents the depth of O_2 penetration.

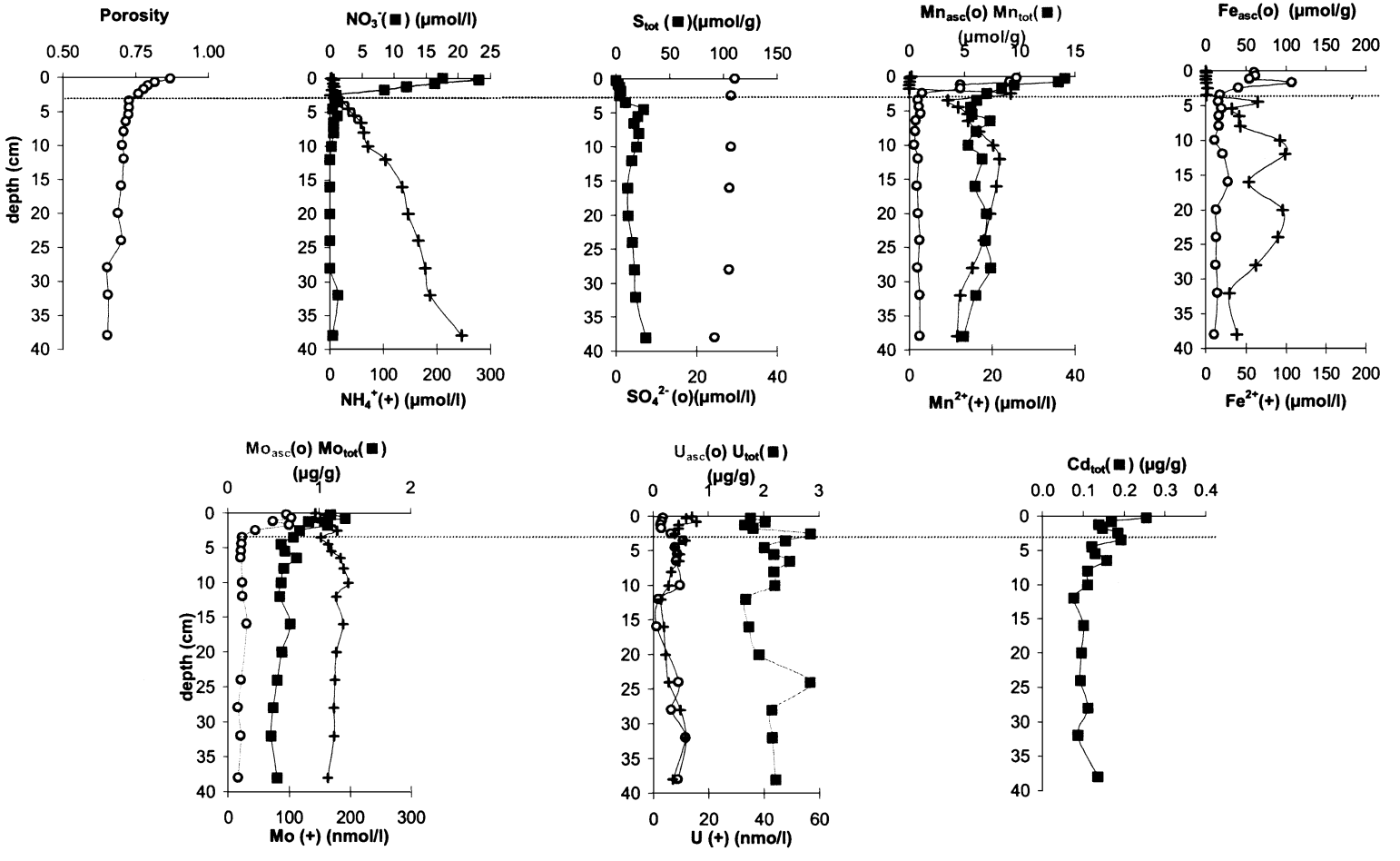

Fig. 6. Vertical distribution of redox species in pore waters and in the solid fraction as determined from total digestion and ascorbate leaching in the core of station B (550 m). The dashed line represents the depth of O_2 penetration.

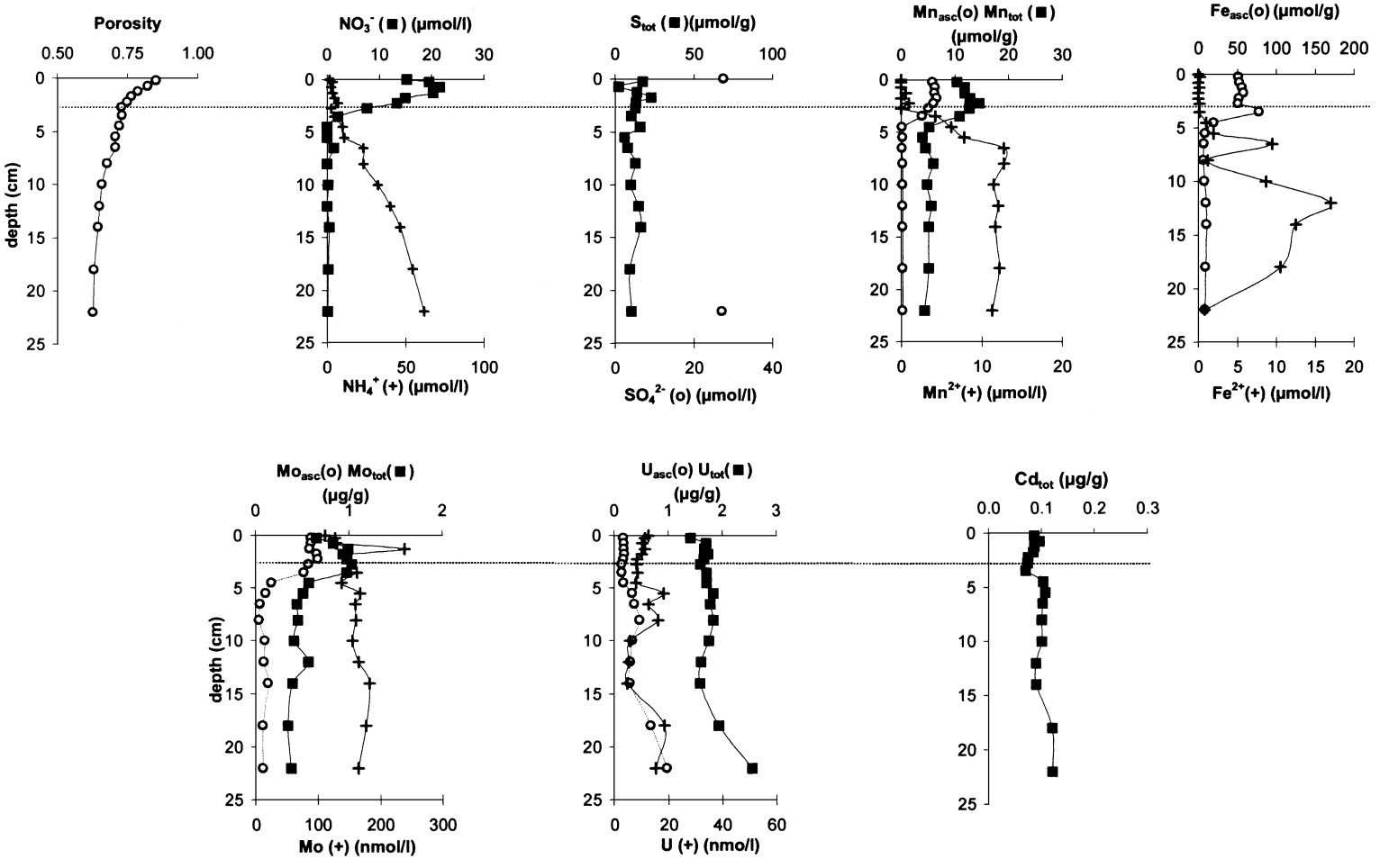

Fig. 7. Vertical distribution of redox species in pore waters and in the solid fraction as determined from total digestion and ascorbate leaching in the core of station A (1000 m). The dashed line represents the depth of O_2 penetration.

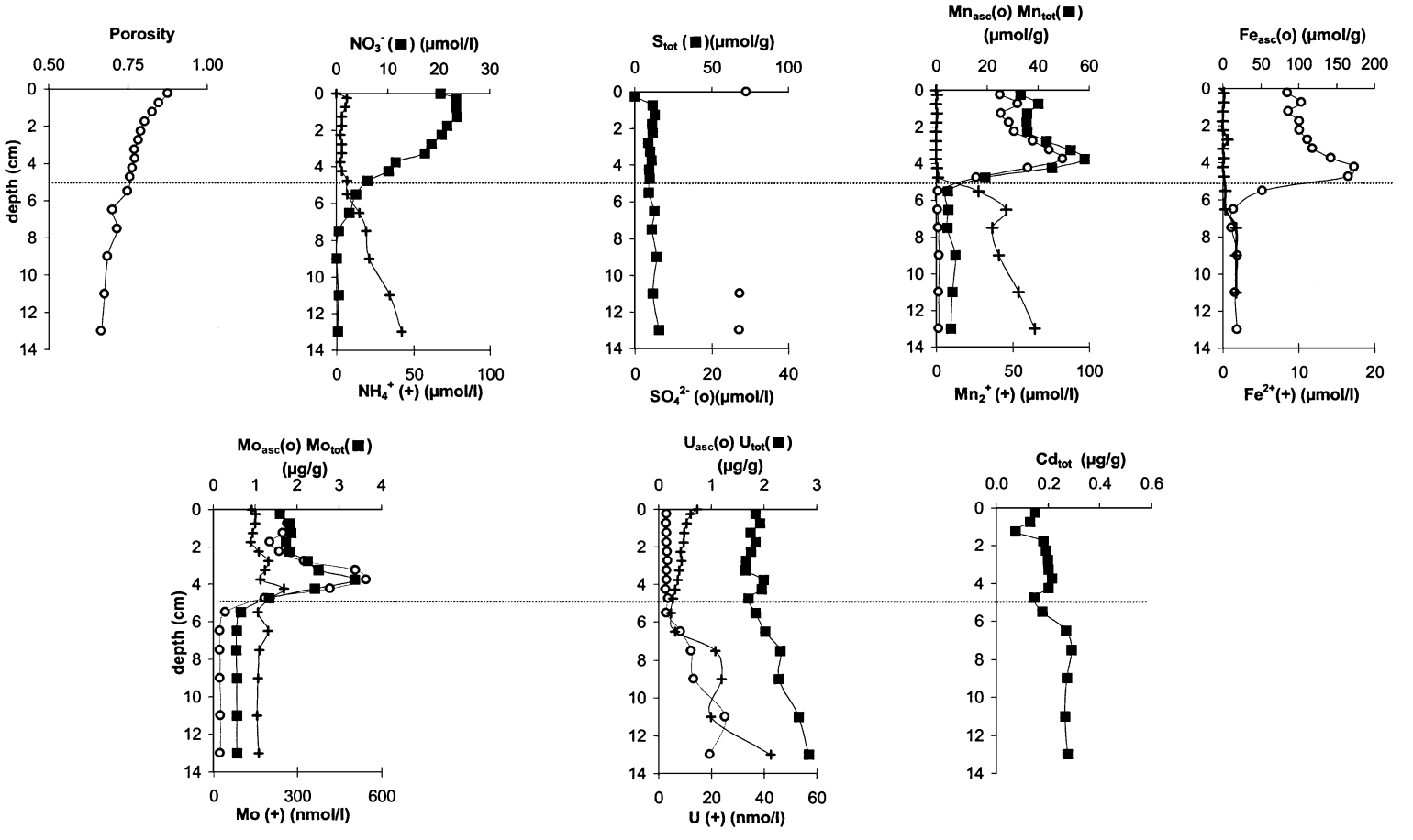

Fig. 8. Vertical distribution of redox species in pore waters and in the solid fraction as determined from total digestion and ascorbate leaching in the core of station I (2800 m). The dashed line represents the depth of O_2 penetration.

bacterial denitrification. Ammonia is produced from anaerobic mineralization of organic N. The addition of dissolved Mn^{2+} and Fe^{2+} in anaerobic sediments is attributed to dissimilatory reduction of Mn- and Fe-oxides by bacteria. The peak of particulate Mn extracted by ascorbate can be attributed to detrital Mn-oxides and authigenic Mn-oxides precipitated from the oxidation of dissolved Mn^{2+} that diffuses from below (Sundby, 1977). In the sediment of stations I, A, and B, the concentration of Mn_{asc} decreases abruptly below the oxic front, reaching values close to zero, which indicates that the Mn-oxides are totally reduced. At station D, concentrations decrease more gradually, probably as the consequence of sediment mixing by bioturbation.

The concentration of Fe_{asc} is highest near the oxic layer and decreases below. Amorphous oxide phases may be used as terminal electron acceptors in bacterial oxidation of organic carbon or they may react with reduced sulfur to form FeS. The first hypothesis is supported by the occurrence of a peak of dissolved Fe (II) at the depth where Fe_{asc} decreases. However, Fe from FeS can be extracted with the ascorbate solution. This may explain the presence of Fe_{asc} in the anoxic part of the cores. This fraction can also consist of a less reactive fraction toward bacterial reduction of Fe-oxides (Postma and Jakobsen, 1996).

At each of the four stations, the lowest solid sulfur concentrations were measured in the sediment surface layer. Stations A and I contained less than 20 μmol/g of S_{tot} and the values remained relatively constant with depth. Station B showed an enrichment of S_{tot} at 5 cm depth, which did not exceed 30 μmol/g. The concentrations in the core of station D increased with depth and reached values higher than 100 μmol/g (Figs. 5–8). The presence of particulate sulfur in continental margin sediments can be mostly attributed to authigenic iron sulfide minerals that precipitate during the degradation of organic matter by sulfate reduction (Berner, 1980; Jørgensen, 1982). The diluted presence of FeS in the deep sediments of stations I, A, and B was confirmed by the presence of small black dots at the surface of the deeper sediment slices. At station D, the presence of FeS was confirmed by the black or dark grey colour below 5 cm depth, and by the characteristic odour of H_2S that emanated when a solution of 1 N HCl was poured on sediment subsamples.

The explanations for the distribution of the major redox species confirm these proposed for cores collected 6 months earlier at comparable stations (Hyacinthe et al., 2001). Some additional reaction pathways have been considered to explain the profiles of Fe, Mn, and N species. These reactions deal with the Mn-oxide reduction by NH_4^+, aerobic denitrification and oxidation of dissolved Fe (II) by NO_3^- or Mn-oxides (Hyacinthe et al., 2001).

3.3. Trace metals: Mo, U, and Cd

Uranium, cadmium, and molybdenum are sensitive to redox changes. These metals are known to be soluble in oxygenated conditions and to precipitate immediately where post-oxic conditions are encountered (Thomson et al., 2001). Under anoxic or suboxic conditions, Mo (VI) is reduced to Mo (IV) (e.g. Bertine, 1972; Malcolm, 1985; Calvert and Pedersen, 1993; Martinez, 1997), and U (VI) to U (IV) (Cochran et al., 1986; Klinkhammer and Palmer, 1991; Calvert and Pedersen, 1993; Thomson et al., 2001). Molybdenum (IV) and U (IV) form poorly soluble precipitates. Cadmium does not change oxidation state, but in the presence of H_2S, it is usually removed from solution as insoluble CdS (Pedersen et al., 1989; Calvert and Pedersen, 1993). The redox layers in the studied sediments have been defined using major redox species and can be used to refine our understanding of the authigenesis of trace metals.

3.3.1. Molybdenum

The total content of particulate Mo (Mo_{tot}) in the surficial samples is 1 μg/g at stations D and B, 0.65 μg/g at station A, and 1.59 μg/g at station I (Figs. 5–8), which is relatively similar to the detrital background values assessed to 1.1 μg/g (Manheim and Landergren, 1978). For the three deepest cores, we observed a subsurface enrichment. The Mo_{tot} values reached 3.36 μg/g at 3.75 cm at station I, and 1.03 μg/g at 2.75 cm at station A. At station B, a maximum of 1.28 μg/g was located in the first centimetre below the interface. Particulate Mo parallels the distribution of ascorbate extractable Mn. Molybdenum in the oxic layer appears therefore to be linked to Mn-oxides. Molybdate (MoO_4^{2-}), the soluble form of Mo in oxic seawater, is adsorbed by Mn-oxides and preferentially by MnO_2 (Shimmield and Price, 1986; Calvert and

Pedersen, 1993). Shimmield and Price (1986) and Martinez (1997) have shown that the Mo/Mn ratio in hemipelagic oxic sediments is close to 0.002, which may reflect co-precipitation or adsorption equilibrium of Mo on MnO_2. We obtain the same ratio in the oxic sediments at stations B, A, and I. Therefore, the Mo enrichment at the surface is most probably linked to Mn-oxide enrichment. Below the Mn-redox boundary, Mo_{tot} values remained constant and were similar (0.4–0.5 μg/g) at the stations B, A, and I, which can be considered as the crustal level value in the three cores. Molybdenum extracted by ascorbate (Mo_{asc}) remained parallel with the Mn_{asc} profile and corresponded to the total Mo minus the estimated crustal values (0.4 μg/g) (Figs. 6–8).

The bottom water concentrations of Mo was between 112 and 144 nmol/l at stations I, A, and B, which was close to, but higher than the average sea water value estimated at 103 nmol/l (Martin and Whitfield, 1983). The concentrations of dissolved Mo increased within the first centimetres of the cores and remained approximately vertical below, with concentrations between 160 and 190 nmol/l. The Mo_{asc} content decreased and became close to zero below the oxic front. Molybdenum was probably released into pore water during the reduction of Mn-oxides (Malcolm, 1985). This agrees with the higher pore water Mo concentration in the anoxic part of the sediment (Figs. 5–8). If we consider that sedimentary authigenic Mo is defined as Mo enrichment over its detrital background value, there is no detectable authigenesis of Mo in the first decimetres of the anoxic part of the stations I, A, and B. There is thus no relationship between Mo accumulation in the oxic layer and Mo accumulation at depth. Consequently, the sedimentary record of Mo does not allow environmental differences to be distinguished among the three stations I, A, and B, even though the C_{org} flux varies by a factor of ~ 2.5, and the O_2 penetration depth varies from 20 to 50 mm.

Station D exhibited no significant maximum of particulate total Mo at the sediment surface below which the Mo content increased gradually, reaching 1.83 μg/g at 36 cm. The thin oxic layer of the station exhibited a weak maximum of Mo_{asc} at the surface, which corresponded to the peak of Mn_{asc}. Below 7 cm depth, the concentration of Mo_{asc} increased. This increase was parallel to the profile of S_{tot} in this core. Anoxic molybdenum authigenesis occurs only at the station D where reduced S is present in high concentrations. The master variable regulating Mo precipitation thus could be the production of sulfides. A threshold value of 0.1 μM dissolved sulfide seems to be prerequisite for the formation of the onset of authigenic Mo–S co-precipitation (Zheng et al., 2000). This suggests that the rate of H_2S or FeS production is sufficiently high at station D to precipitate Mo as sulfide minerals, with or without Fe. Sulfide content was low or not detectable in the other cores, which may explain the lack of Mo authigenesis in the anoxic part of sediments. Several studies have shown that Mo may form a separate insoluble sulfide phase, possibly MoS_3 or MoS_2, when FeS is converted to pyrite (Shimmield and Pedersen, 1990; Calvert and Pedersen, 1993). Molybdenum enrichment did not appear abruptly below the redox front. Molybdenum concentrations increased progressively with depth, probably due to the transport of Mo-bearing particles, such as Mn-oxides, deep in the sediment by bioturbation. Molybdenum can be released into pore water due to Mn-oxide reduction and directly be trapped with reduced sulfur forming Mo–Fe–S by co-precipitation or directly MoS_2 or MoS_3. This process can smooth the Mo signal in the entire mixed layer, as observed.

At station D, dissolved Mo concentrations decreased slightly in the thin oxic layer, from 189 nmol/l, which was the bottom water value, to 146 nmol/l. Then, the concentration remained approximately constant down to 7 cm depth. Below, Mo concentrations were higher and more variable. The depth of 7 cm corresponded to several changes in sediment chemistry. Mo_{asc} increased below this depth. Ammonia also increased abruptly, whereas dissolved Fe^{2+} dropped to low concentrations. At this depth, Mn_{asc} also decreased (Fig. 5). All these observations can be combined together in the following scenario: Mn-oxides extracted with the ascorbate solution are present in the anoxic sediment down to 7 cm because of the sediment mixing by bioturbation, which is important at station D. Dissolved sulfide cannot reach high concentrations in this layer, because Mn-oxides are efficient oxidizing species for reduced sulfur (Aller and Rude, 1988). Therefore, within this upper part of the anoxic sediment, Mo cannot precipitate as Mo–S species and the distribution of particulate and soluble Mo must be controlled by Mn-oxides. Below 7 cm,

dissolved sulfide from sulfate reduction probably appears and triggers dissolved Fe concentrations to low values due to iron sulfide precipitation. Authigenic Mo probably co-precipitates with FeS at this depth. Therefore, at station D, the depth of authigenic Mo precipitation seems to be controlled by bioturbation.

The concentration of dissolved Mo increased in the deeper part of the sediment core of station D. Therefore, the gradual increase of solid Mo below 7 cm can be due to the availability of dissolved Mo for precipitation throughout the length of the core. The occurrence of irregularities and the high concentration of Mo in the pore water has been observed in several other studies (Shaw et al., 1990; Zheng et al., 2000) and remain a matter of debate. Zheng et al. (2000) suggested that several factors could contribute to this pore water Mo: (1) the relaxation of Mo from previous more reducing conditions, (2) the presence of microzones of Mo precipitation due to the sulfate reduction and oxidation of sulfide in these areas, or (3) sampling artefacts. In our study, it is possible that during the release of Mo by Mn-oxides advected by bioturbation below the oxic layer, some parts of the Mo remain as MoO^{2+} before precipitation with S. Nevertheless, we cannot exclude the hypothesis of oxidation and redissolution of reduced particulate Mo during the sampling of pore waters. We have calculated that a redissolution of 1:1000 of the particulate Mo can explain the concentration of dissolved Mo we measured.

3.3.2. Uranium

The concentrations of total U (U_{tot}) ranged between 1.5 and 2 μg/g in the core tops (Figs. 5–8). These values are below the mean value of 2.7 μg/g in hemipelagic sediments (Colley and Thomson, 1985; Thomson et al., 1990). We noted an increase of the concentrations to 2 or 3 μg/g at the bottom of the four cores. The concentration at the bottom of the deepest core I was equal to that measured at the bottom of the shallowest core D (2.85 μg/g). The profiles of U extracted by the ascorbate solution (U_{asc}) showed lower concentrations and were less noisy than U_{tot}. At stations I, A, and B, the concentration of U_{asc} remained constant between 0.1 and 0.2 μg/g in the top part of the cores. This layer was thicker than the oxic layer and corresponded to the area enriched in Fe_{asc}. U_{asc} concentrations increased to 0.4–0.5 μg/g just below the Fe_{asc}-enriched area. Below, the U_{asc} content remained relatively constant, except for some samples at the bottom of the cores, which reached 1 μg/g. The U_{asc} content of the sediment from station D was above 0.2 μg/g at the top and increased gradually to 0.53 μg/g at the bottom of the core.

The subsurface enrichment of U_{asc} in the four cores suggests authigenic U precipitation in the anoxic zone of the sediment. The carbonate complex $UO_2(CO_3)_3^{4-}$ is the soluble stable U (VI) species in oxic marine sediments (Langmuir, 1978). Under reducing conditions, U (VI) is reduced to much less soluble U (IV) or U (V), which may then precipitate as UO_2, U_3O_7, or U_3O_8, or be adsorbed on the surface of existing minerals (Langmuir, 1978; Kniewald and Branica, 1988; Anderson et al., 1989). The redox potential at which the U (VI) to U (IV) transition occurs is close to that of the reduction of Fe (III) to Fe (II) at the pH and alkalinity of seawater. Langmuir (1978) suggested that HS created during sulfate reduction could be a reducing agent for U (VI). Dissimilatory bacterial reduction of U in the presence of Fe (III) and sulfate was also suggested (Lovley et al., 1991; Fredrickson et al., 2000). However, all cores (D, B, A, and I) showed U authigenesis although the content of authigenic S was low or undetectable at stations I, A, and B, whereas it was high at station D. We also noted that the U content at the bottom of the cores was similar, between 2.2 and 2.9 μg/g. Consequently, in these sediments, the concentration of authigenic U appeared to be independent of sulfide authigenesis.

The dissolved U content in the bottom water was close to 14 nmol/l, which is the global seawater value (Cochran et al., 1986; Klinkhammer and Palmer, 1991). In all cores, we noted a decrease of dissolved U from the bottom water to the depth where U_{asc} exceeded 0.2 μg/g. The minimal concentration of dissolved U measured at this depth is far from zero. At station I, where the oxic layer is the most extended, the dissolved U profile showed a very smooth decrease from 0 to 6 cm, which can be interpreted as a diffusion profile of U from the seawater to the depth where U is removed. The minimum concentration of dissolved U at 6 cm is 4.7 nmol/l, and not 0, which indicates that the removal of dissolved U is not total. We observed the same pattern in the sediment of the other stations, where the smooth gradient of dissolved U is restricted to a thinner layer. These profiles can be used to estimate

the flux of U by molecular diffusion from the water column to the minimum value assuming steady state conditions. The diffusive flux can be calculated from the concentration gradients according to Fick's first law:

$$J = -\phi \times \mathrm{Ds} \times \Delta C/\Delta Z$$

where J is the flux (negative J values correspond to downward fluxes, and positive J values to upward fluxes), ϕ is the porosity, $\Delta C/\Delta Z$ is the concentration gradient, and Ds is the bulk sediment diffusion coefficient corrected for tortuosity, i.e. $\mathrm{Ds} = D_0/\theta^2$, where θ is the tortuosity and D_0 is the molecular diffusion coefficient in water (Berner, 1980). D_0 value was calculated from the tabulated value for the uranyl ion from Li and Gregory (1974) corrected for the temperature of the bottom water at the moment of sampling; the value of θ^2 is assumed to be equal to $1 - \ln(\phi^2)$ (Boudreau, 1996). We have used the concentration gradient between the bottom water sample (14, 13, and 15 nmol/l for B, A, and I, respectively) and the minimal value located below the oxic front. We obtain downward fluxes of -71, -110, and -170 pmol/cm^2/year for stations I, A, and B, respectively. The theoretical enrichment of U in the solid fraction due to diffusion can be estimated from the ratio of the diffusive flux and accumulation rate of the particles. The calculated enrichment of U corresponds to a minimal value, because the accumulation rate obtained by the $^{210}Pb_{xs}$ activity corresponds to a maximal value. We obtain 1.00, 0.73, and 0.51 μg/g for the stations I, A, and B, respectively. These calculated values are higher than enrichment of U_{asc} measured at the top of the anoxic layer, but they correspond to the enrichment of authigenic U at the bottom of the cores. Therefore, the content of fossilised authigenic U is consistent with the flux of U from seawater down into the sediment estimated by a diffusion model at steady state, as proposed by Barnes and Cochran (1988), Anderson et al. (1989), and Thomson et al. (2001). However, the mechanism of particulate U enrichment is more complex than direct reductive precipitation at the oxic/anoxic boundary.

Dissolved U becomes important in the anoxic part of the sediment for all stations, where it is supposed to become insoluble. This anoxic enrichment exceeds the U concentration in the overlying water, at station D, for example, the dissolved U content reached 40 nmol/l near the bottom of the core. The presence of high dissolved U concentration in anoxic sediments has also been reported in many other studies (e.g. Kolodny and Kaplan, 1973; Anderson et al., 1989). The authors interpret this concentrations as caused by weak re-oxygenation of the sediment during handling and the partial conversion of U (IV) to U (VI). We cannot exclude this hypothesis as explanation of our profiles, because solid U-phase in reducing environment is readily oxidised and mobilised into solution by air contamination during the water extraction (Anderson, 1984; Thomson et al., 1990). In our samples, the oxidation of less than 1% of authigenic U could explain the pore water value. Moreover, an in situ increase of dissolved U in the anoxic zone should trigger a diffusive upward flux of U toward the redox boundary, which should produce a solid phase maximum. Such a maximum is not observed. It is also possible that the pore water U measured in the anoxic sediment comes from an authigenic colloidal fraction that crossed the 0.2-μm pore size filter used to define the "dissolved fraction".

At each of the four stations, authigenic U was not constant in the anoxic sediment and increased with depth as observed in other studies (Thomson et al., 1990, 2000; Barnes and Cochran, 1993). No steady-state conditions could explain the increase. As for Mo, bioturbation could also explain the distribution of U. In this case, U is scavenged in the oxic zone from a particulate phase derived from the anoxic layer. Kolodny and Kaplan (1973) reported that U (VI) can be scavenged by particulate organic carbon in the oxic layer, and Anderson (1982) has identify U (VI)–organic matter association (adsorption or complexation) in sediment trap. These carrier phases could be preserved and could retain complexed U (VI), which could be released in more reducing conditions. Barnes and Cochran (1993) suggested that U could be scavenged by Fe-oxides. However, we have not detected significant ascorbate extractable U in the oxic part of the cores.

3.3.3. Cadmium

The Cd extracted by ascorbate and dissolved Cd concentrations were below detection limit for all studied stations. The total particulate cadmium concentrations ranged from 0.1 to 0.3 μg/g at the top of

the cores. These values were close to the crustal values estimated at 0.1 μg/g (Taylor and McLennan, 1985). All profiles of total Cd exhibited a decrease just below the sediment/water interface. The biogeochemistry of Cd is dominated by the cycle of organic matter (Boyle et al., 1976). Klinkhammer et al. (1982) and Gendron et al. (1986) have suggested that the decrease of particulate Cd near the water/sediment interface was the consequence of the oxic degradation of fresh organic matter, in which Cd is incorporated. This process could explain the upper part of our profiles and suggests that the top of the sediment column was a source of dissolved Cd for the bottom waters and the underlying anoxic sediment.

Particulate Cd increased abruptly below the oxic front at stations I and A. The sediment of station B did not show a significant enrichment of Cd below the oxic/anoxic interface, probably because the concentrations in the oxic part remained high, but the concentration of particulate Cd measured in the anoxic sediment of station B and A was the same (0.1 μg/g). At station D, Cd increased gradually with depth, and reached 0.52 μg/g at the bottom of the core.

The enrichment of Cd was likely due to the precipitation of highly insoluble CdS, which can occur in the presence of very low H_2S concentrations, as observed by Lapp and Balzer (1993). This suggests that sulfate reduction occurred in all the studied cores. This is obvious for station D, where solid phase S increased with depth at the same time as dissolved SO_4^{2-} decreased. The Cd profile followed the S profile at this station. In other cores, the concentration of solid phase of S was low. At station B, solid phase S increases below 4 cm, but at stations A and I, there was no obvious accumulation of sulfur. However, NH_4^+ was present in the pore water at all stations, increasing with depth. Ammonia is the product of the anaerobic degradation of organic nitrogen. At stations A and I, the ammonia concentration was lower than at stations B and D, but reached 40 μmol/l at 12 cm depth. Ammonia production probably reflected organic matter degradation by sulfate reduction, which may have produced enough sulfide to trap Cd. Cadmium appears to be a sensitive indicator of SO_4^{2-} reduction.

The depth at which particulate Cd increased was just below the Mn-oxide containing layer. The contrast between the vertical distribution of Mn and Cd was clearly demonstrated at stations I and A. Gobeil et al. (1997) showed that the depth interval between the particulate Mn-oxide maximum and the Cd maximum corresponded to the minimum and the maximum depth of O_2 penetration, respectively, during redox front oscillation. At stations A and I, this depth interval was approximately 1.5 cm. This may represent the seasonal oscillation of the depth of the oxic layer caused by the intermittent flux of labile organic matter.

3.4. The sedimentary signal of Mo, Cd, and U

The fundamental interest of paleoceanographic studies is to reconstruct the temporal evolution of oceanographic parameters, such as the bottom water oxygen concentration or primary productivity by way of exported production. Sediment depth in the sediment is considered to be a measure of time since deposition. Molybdenum, Cd, and U are used as markers of surficial redox conditions. Their use is based on the hypothesis that the flux of a species from the bottom water to the anoxic sediment and the rate of fixation below the oxic/anoxic boundary increases when the flux of exported organic mater increases itself, i.e. when the oxic/anoxic boundary rises. Theoretically, the sharper the gradient, the greater the accumulation of the authigenic phase. This is not true for all environments. Stations I, A, and B are different in terms of organic carbon flux and O_2 penetration depth, and yet we observe only minor differences between the distribution of the three trace metals in the anoxic layer of the cores.

Molybdenum is enriched in the most reducing sedimentary environment when solid S is enriched (station D). Only in this situation can the linkage of authigenic formation with sulfide be exploited for paleo-reconstructions. No such enrichment is observed in the cores of stations I, A, and B. Thus, the sedimentary record of Mo does not distinguish between the three stations. Where the bottom water is well oxygenated, Mo is therefore not a discriminating indicator of exported production. Cadmium enrichment indicates that sulfate reduction occurs, and permits even a better resolution than Mo or S.

Contrary to Mo and Cd, the precipitation of U (IV) appears to be independent of the sulfide authigenesis. The authigenesis of U can be described by a diffusive flux model and authigenic U appears to have a sea

water source. The profiles of stations I, A, and B show that the flux of U is controlled by the thickness of the oxic layer. Uranium begins to be fixed in the presence of reducing environment, below the oxic/anoxic boundary. However, the definite depth of U precipitation is not equal to three times the depth of O_2 penetration as suggested by Crusius and Thomson (1999), but it corresponds to a broad layer of enrichment that occurs gradually below the Fe_{asc} reduction. Therefore, it is difficult to use authigenic U retroactively to estimate the depth of the oxic/anoxic boundary in sediments. Moreover, this phenomenon tends to create a vertical gap between the recorded signal and the sediment/water interface. Therefore, this effect can bias dating scales of paleoclimatic trace metals records. Station D shows that the relation between authigenic metal concentration and the depth of precipitation is even more complex when this depth is located within the layer mixed by bioturbation.

4. Conclusions

We have described the geochemical distribution of Mo, U, and Cd in modern sediments of the Bay of Biscay in relation to the distribution of major redox species (dissolved O_2, NO_3^-, NH_4^+, Mn, and Fe, and particulate S, C_{org}, Mn- and Fe-oxides). The sediments at the shallowest station are enriched in organic carbon and sulfide minerals and are highly bioturbated. The sediments at the three deeper stations are much less bioturbated and organic carbon levels are lower. In all sites, early diagenesis follows the depth sequence of redox reactions established by Froelich et al. (1979).

The vertical distribution of the trace metals is often related to the presence of major phases. Authigenic Mo and U were successfully extracted with an ascorbate solution. Molybdenum is associated with Mn-oxides in the oxic layer of cores. In the anoxic layer, Mo is precipitated as a detectable authigenic phase only when sulfide minerals are abundant, i.e. when sulfate reduction is important. Molybdenum and sulfur give the same information.

Particulate Cd is depleted just below the sediment/water interface due to oxic degradation of organic matter and subsequent release of Cd to the pore water. In the anoxic sediments, in the four studied cores, Cd enrichment seems to be a good indicator of sulfide production.

No relationship was observed between U and S. Uranium begins to precipitate at the depth where reduction of reactive iron (III) occurs. The U concentration at this depth is lower than the minimum values calculated from estimated accumulation rates and a downward diffusive flux of dissolved U from the bottom seawater. However, authigenic U concentrations continue to increase in the anoxic part of the cores. The downward flux of dissolved U to form authigenic enrichment appears to be controlled by the redox conditions at the water/sediment interface (downward flux of O_2 from bottom water and both quality and quantity of exported organic matter) but U immobilization requires probably a multistep reduction with slow kinetics at one or more of the electron reactions.

Acknowledgements

This research was funded by the program PROOF of the Institut National des Sciences de l'Univers and by a Marie Curie fellowship of the European Community programme "Energy, Environment and Sustainable Development" under contract number EVK1-CT-2000-5003. We gratefully acknowledge the assistance of the crew of the "Côte de la Manche" and the participants of the Oxybent missions. We would like to express our gratitude to Philippe Martinez, Jean-Marie Jouanneau, Karine Dedieu, and Hervé Derriennic who have contributed in different ways to this works. We would also like to thank Bjørn Sundby for his helpful comments on the manuscript. Drs. P. Santschi, J. Bruno, and three anonymous reviewers are gratefully acknowledged for their useful comments and suggestions. This is the contribution No. 1426 of the UMR 5805 EPOC.

Associate editor: Dr. Peter Santschi.

References

Aller, R.C., Rude, P.D., 1988. Complete oxidation of solid phase sulfide by manganese and bacteria in anoxic marine sediments. Geochim. Cosmochim. Acta 52, 751–765.

Aller, R.C., Hall, P.O.J., Rude, P.D., Aller, J.Y., 1998. Biogeochemical heterogeneity and suboxic diagenesis in hemipelagic sediments of the Panama Basin. Deep-Sea Res., Part 1 45, 133–165.

Anderson, L., 1979. Simultaneous spectrophotometric determination of nitrite and nitrate by flow injection analysis. Anal. Chim. Acta 110, 123–128.

Anderson, R.F., 1982. Concentrations, vertical flux and remineralization of particulate uranium in seawater. Geochim. Cosmochim. Acta 46, 1293–1299.

Anderson, R.F., 1984. A method for determining the oxidation state of uranium in natural waters. Nucl. Instrum. Methods Phys. Res. 233, 213–217.

Anderson, R.F., LeHuray, A.P., Fleisher, M.Q., Murray, J.W., 1989. Uranium deposition in Saanich Inlet sediments, Vancouver Island. Geochim. Cosmochim. Acta 53, 2205–2213.

Anschutz, P., Zhong, S., Sundby, B., Mucci, A., Gobeil, C., 1998. Burial efficiency of phosphorus and the geochemistry of iron in continental margin sediments. Limnol. Oceanogr. 43, 53–64.

Anschutz, P., Hyacinthe, C., Jouanneau, J.M., Jorissen, F.J., 1999. La distribution du phosphore inorganique dans les sédiments modernes du Golfe de Gascogne. C. R. Acad. Sci. 328, 765–771.

Anschutz, P., Sundby, B., Lefrançois, L., Luther III, G.W., Mucci, A., 2000. Interaction between metal oxides and nitrogen and iodine in bioturbated marine sediments. Geochim. Cosmochim. Acta 64, 2751–2763.

Barnes, C.E., Cochran, J.K., 1988. The geochemistry of uranium in marine sediments. In: Guary, J.C., Guegueniat, P., Pentreath, R.J. (Eds.), Radionucleides: A Tool for Oceanography. Elsevier, London, pp. 162–170.

Barnes, C.E., Cochran, J.K., 1993. Uranium geochemistry in estuarine sediments: controls on removal and release processes. Geochim. Cosmochim. Acta 57, 555–569.

Berner, R.A., 1980. Early Diagenesis: Theoretical Approach. In: Holland, H.D. (Ed.), Princeton Series in Geochemistry, Princeton Univ. Press, Princeton, 241 pp.

Bertine, K.K., 1972. The deposition of molybdenum in anoxic waters. Mar. Chem. 1, 43–53.

Boudreau, B.P., 1996. The diffusive tortuosity of fine-grained unlithified sediments. Geochim. Cosmochim. Acta 60, 3139–3142.

Boyle, E.A., Sclater, F., Edlong, J.M., 1976. On the marine geochemistry of Cd. Nature 263, 42–44.

Calvert, S.E., 1987. Oceanographic controls on the accumulation of organic matter in marine sediments. In: Brooks, J., Fleet, A.J. (Eds.), Marine Petroleum Source Rocks.Geol. Soc. London Spec. Publ.

Calvert, S.E., Pedersen, T.F., 1993. Geochemistry of recent and anoxic marine sediments: implication for the geological records. Mar. Geol. 113, 67–88.

Canfield, D.E., Jørgensen, B.B., Fossing, H., Glud, R., Gundersen, J., Ramsing, N.B., Thamdrup, B., Hansen, J.W., Nielsen, L.P., Hall, P.O.J., 1993. Pathways of organic carbon oxidation in three continental margin sediments. Mar. Geol. 113, 27–40.

Cochran, J.K., Carey, A.E., Sholkovitz, E.R., Surprenant, L.D., 1986. The geochemistry of uranium and thorium in coastal marine sediment pore waters. Geochim. Cosmochim. Acta 50, 663–680.

Colley, S., Thomson, J., 1985. Recurrent uranium relocations in distal turbidites emplaced in pelagic conditions. Geochim. Cosmochim. Acta 49, 2339–2348.

Crusius, J., Thomson, J., 1999. Comparative behavior of authigenic Re, U and Mo during reoxidation and subsequent long-term burial in marine sediments. Geochim. Cosmochim. Acta 64, 2233–2242.

François, R., 1988. A study on the regulation of the concentration of some trace metals (Rb, Sr, Pb, Cu, V, Cr, Ni, Mn and Mo) in Saanich Inlet sediments, British Columbia, Canada. Mar. Geol. 83, 285–308.

Fredrickson, J.K., Zachara, J.M., Kennedy, D.W., Duff, M.C., Gorby, Y.A., Li, S.W., Krupka, K.M., 2000. Reduction of U (VI) in goethite (α-FeOOH) suspension by a dissimilatory metal-reducing bacterium. Geochim. Cosmochim. Acta 64, 3085–3098.

Froelich, P.N., Klinkhammer, G.P., Bender, M.L., Luedke, N.A., Heath, G.R., Cullen, D., Dauphin, P., Hammond, D., Hartman, B., Maynard, V., 1979. Early oxidation of organic matter in pelagic sediments of the Eastern Equatorial Atlantic: suboxic diagenesis. Geochim. Cosmochim. Acta 43, 1075–1090.

Gendron, A., Silverberg, N., Sundby, B., Lebel, J., 1986. Early diagenesis of cadmium and cobalt of the Laurentian Trough. Geochim. Cosmochim. Acta 50, 741–747.

Gobeil, C., Silverberg, N., Sundby, B., Cossa, D., 1987. Cadmium diagenesis in Laurentian Trough sediments. Geochim. Cosmochim. Acta 51, 589–596.

Gobeil, C., Macdonald, R.W., Sundby, B., 1997. Diagenetic separation of cadmium and manganese in suboxic continental margin sediments. Geochim. Cosmochim. Acta 61, 4647–4654.

Hall, P.O.J., Aller, R.C., 1992. Rapid, small-volume flow injection analysis for CO_2 and NH_4^+ in marine and freshwaters. Limnol. Oceanogr. 30, 1113–1119.

Helder, W., Backer, J.F., 1985. Shipboard comparison of micro- and mini electrodes for measuring oxygen distribution in marine sediments. Limnol. Oceanogr. 30, 1106–1109.

Hulth, S., Aller, R.C., Gibert, F., 1999. Coupled anoxic nitrification/manganese reduction in marine sediments. Geochim. Cosmochim. Acta 63, 49–66.

Hyacinthe, C., Anschutz, P., Jouanneau, J.M., Jorissen, F.J., 2001. Early diagenesis processes in the muddy sediment of the Bay of Biscay. Mar. Geol. 177, 111–128.

Jørgensen, B.B., 1982. Mineralization of organic matter in the seabed. The role of the sulfate reduction. Nature 296, 643–645.

Jouanneau, J.M., Garcia, C., Oliviera, A., Rodrigues, A., Dias, J.A., Weber, O., 1988. Dispersal and deposition of suspended sediment on the shelf off the Tagus and Sado estuaries, SW Portugal. Prog. Oceanogr. 42 (1–4), 233–257.

Klinkhammer, G.P., Palmer, M.R., 1991. Uranium in the oceans: where it goes and why. Geochim. Cosmochim. Acta 55, 1799–1806.

Klinkhammer, D., Heggie, D.T., Graham, D.W., 1982. Metal diagenesis in oxic marine sediments. Earth Planet. Sci. Lett. 61, 65–76.

Kniewald, G., Branica, M., 1988. Role of the uranium (V) in marine sedimentary environment: a geochemical possibility. Mar. Chem. 24, 1–12.

Kolodny, Y., Kaplan, I.R., 1973. Deposition of uranium in the sediment and interstitial water of an anoxic fjord. In: Ingerson, E. (Ed.), Symp. Hydrogeochemistry. Clarke, Washington, DC, pp. 418–442.

Kostka, J.E., Luther III, G.W., 1994. Portioning and speciation of solid phase iron in saltmarsh sediments. Geochim. Cosmochim. Acta 58, 1701–1710.

Langmuir, D., 1978. Uranium solution-mineral equilibrium at a low temperatures with applications to sedimentary ore deposits. Geochim. Cosmochim. Acta 42, 547–569.

Lapp, B., Balzer, W., 1993. Early diagenesis of trace metals used an indicator of past productivity changes in coastal sediments. Geochim. Cosmochim. Acta 57, 4639–4652.

Li, Y.H., Gregory, S., 1974. Diffusion of ions in seawater and in deep-sea sediments. Geochim. Cosmochim. Acta 38, 703–714.

Loring, D.H., Rantala, R.T.T., 1992. Manual for the geochemical analysis of marine sediment and suspended particulate matter. Earth Sci. Rev. 32, 235–283.

Lovley, D.R., Phillips, E.P.J., Gorby, Y.A., Landa, R.L., 1991. Microbial reduction of uranium. Nature 350, 413–416.

Malcolm, S.J., 1985. Early diagenesis of molybdenum in estuarine sediments. Mar. Chem. 16, 213–225.

Manheim, F.T., Landergren, S., 1978. Handbook of Geochemistry II. Section 42. B–O. Springer-Verlag, Berlin.

Martin, J.M., Whitfield, M., 1983. The significance of the river input of chemical elements to the ocean. In: Wong, C.S., Boyle, E., Bruland, K.W., Burton, J.D., Goldberg, E.D. (Eds.), Trace Metals in the Sea Water. Plenum, New York.

Martinez, P., 1997. Paléoproductivité du système d'upwelling Nord-ouest africain et variations climatiques au cours du Quaternaire terminal. PhD Thesis, Univ. Bordeaux I, France, unpublished.

Martinez, P., Bertrand, P., Calvert, S.E., Pedersen, T.F., Shimmield, G.B., Lallier-Vergès, E., Fontugne, R., 2000. Spatial variations in nutrient utilization, production and diagenesis in sediments of a coastal upwelling regime (NW Africa): implications for the paleoceanographic record. J. Mar. Res. 58, 809–835.

Migeon, S., Weber, O., Faugère, J.C., Saint-Paul, J., 1999. SCOPIX: a new X-ray imaging system for core analysis. Geo Mar. Lett. 18, 251–255.

Pedersen, T.F., Water, R.D., Macdonald, R.W., 1989. On the natural enrichment of cadmium and molybdenum in the sediments of Ucluelet Inlet, British Columbia. Sci. Total Environ. 79, 125–139.

Postma, D., Jakobsen, R., 1996. Redox zonation: equilibrium contains on the Fe(III)/SO_4^{2-} reduction interface. Geochim. Cosmochim. Acta 60, 3169–3175.

Revsbech, N.P., 1983. In-situ measurements of oxygen profiles of sediments by use of oxygen microelectrodes. In: Forstner, G. (Ed.), Polarographic Oxygen Sensors. Springer-Verlag, Berlin, pp. 265–273.

Revsbech, N.P., Jørgensen, B.B., 1986. Microelectrodes: their use in microbial ecology. Advances in Microbial Ecology. Plenum, New York, pp. 293–352.

Rosenthal, Y., Lam, P., Boyle, E.A., Thomson, J., 1995. Authigenic cadmium enrichments in suboxic sediments: precipitation and post depositional mobility. Earth Planet. Sci. Lett. 132, 99–111.

Shaw, T.J., Gieskes, J.M., Jahnke, R.A., 1990. Early diagenesis in differing depositional environments: the response of transition metals in pore water. Geochim. Cosmochim. Acta 54, 1233–1246.

Shimmield, G.B., Pedersen, T.F., 1990. The geochemistry of reactive trace metals and halogens in hemipelagic continental margin sediments. Rev. Aquat. Sci. 3, 255–279.

Shimmield, G.B., Price, N.B., 1986. The behaviour of molybdenum and manganese during early sediment diagenesis—offshore Baja California, Mexico. Mar. Chem. 19, 261–280.

Silverberg, N., Nguyen, H.V., Delibrias, G., Koide, M., Sundby, B., Yokoyama, Y., Chesselet, R., 1986. Radionuclide profiles, sedimentation rates, and bioturbation in modern sediments of Laurentian Trough, Gulf of St. Lawrence. Oceanol. Acta 9, 285–290.

Stookey, L.L., 1970. Ferrozine—a new spectrophotometric reagent for iron. Anal. Chem. 42, 779–781.

Strickland, J.D.H., Parsons, T.R., 1972. A practical handbook of seawater analysis. Bull. Fish. Res. Board Can. 167, 1–31.

Sundby, B., 1977. Manganese-rich particulate matter in coastal marine environment. Nature 270, 417–419.

Taylor, S.R., McLennan, S.M., 1985. In: Oxford (Ed.), The Continental Crust: Its Composition and Evolution. Blackwell Scientific Publications Ltd., London, 312 pp.

Thomson, J., Wallace, H.E., Colley, S., Toole, J., 1990. Authigenic uranium in Atlantic sediments of the last glacial stage—a diagenetic phenomenon. Earth Planet. Sci. Lett. 98, 222–232.

Thomson, J., Brown, L., Nixon, S., Cook, G.T., MacKenzie, A.B., 2000. Bioturbation and holocene sediment accumulation fluxes in the north-east Atlantic Ocean (Benthic Boundary Layer experiment sites). Mar. Geol. 169, 21–39.

Thomson, J., Nixon, S., Croudace, I.W., Pedersen, T.F., Brown, L., Cook, G.T., Mackenzie, A.B., 2001. Redox-sensitive element uptake in north-east Atlantic Ocean sediments (Benthic Boundary Layer Experiment Site). Earth Planet. Sci. Lett. 184, 535–547.

Zheng, Y., Anderson, R.F., Van Geen, A., Kuwabara, J., 2000. Authigenic molybdenum formation in marine sediments: a link to pore water sulphide in the Santa Barbara Basin. Geochim. Cosmochim. Acta 64, 4165–4178.